Identification of chemicals breaking the USP8 interaction with its endocytic substrate CHMP1B

Agnès Journet, Caroline Barette, Laurence Aubry, Emmanuelle Soleilhac, Marie-Odile Fauvarque

SLAS Discovery 27 (2022) 395–404

Contents lists available at ScienceDirect

SLAS Discovery

journal homepage: www.elsevier.com/locate/slasd

Original Research

Identification of chemicals breaking the USP8 interaction with its endocytic substrate CHMP1B

Agnès Journet[a], Caroline Barette[a], Laurence Aubry[b], Emmanuelle Soleilhac[a], Marie-Odile Fauvarque[a,*]

[a] Univ. Grenoble Alpes, CEA, Inserm, IRIG, BGE, F-38000 Grenoble, France
[b] Univ. Grenoble Alpes, CNRS, CEA, Inserm, IRIG, BGE, F-38000 Grenoble, France

ARTICLE INFO

Keywords:
Drug discovery
Endocytosis
High-throughput screening
MIT domain
ESCRT
Protein-protein interaction

ABSTRACT

The ubiquitin-specific protease USP8 plays a major role in controlling the stability and intracellular trafficking of numerous cell surface proteins among which the EGF receptor that regulates cell growth and proliferation in many physio-pathological processes. The function of USP8 at the endocytic pathway level partly relies on binding to and deubiquitination of the Endosomal Sorting Complex Required for Transport (ESCRT) protein CHMP1B. In the aim of finding chemical inhibitors of the USP8::CHMP1B interaction, we performed a high-throughput screening campaign using an HTRF® assay to monitor the interaction directly in lysates of cells co-expressing both partners. The assay was carried out in an automated format to screen the academic Fr-PPIChem library (Bosc N *et al.*, 2020), which includes 10,314 compounds dedicated to the targeting of protein-protein interactions (PPIs). Eleven confirmed hits inhibited the USP8::CHMP1B interaction within a range of 30% to 70% inhibition at 50 μM, while they were inactive on a set of other PPI interfaces demonstrating the feasibility of specifically disrupting this particular interface. In parallel, we adapted this HTRF® assay to compare the USP8 interacting capacity of CHMP1B variants. As anticipated from earlier studies, a deletion of the MIM (Microtubule Interacting and Trafficking domain Interacting Motif) domain or mutation of two conserved leucine residues, L192 and L195, in this domain respectively abolished or strongly impeded the USP8::CHMP1B interaction. By contrast, a CHMP1B mutant that displays a highly decreased ubiquitination level following mutation of four lysine residues in arginine interacted at a similar level as the wild-type form with USP8. Therefore, conserved leucine residues within the MIT domain rather than its ubiquitinated status triggers CHMP1B substrate recognition by USP8.

Introduction

Regulation of cell signaling and response to external stimuli strongly depend on the endocytic process and associated ubiquitination/deubiquitination events. Indeed, many plasma membrane receptors are ubiquitinated following their activation through binding to their cognate ligand leading to their internalization by endocytosis (for review, see [9]). Ubiquitin-driven internalization of receptor is notably documented in the case of receptor tyrosine kinases RTKs such as the Epidermal Growth Factor (EGF) receptor EGFR. Their fate is then highly depending on the action of deubiquitinating enzymes (DUBs), such as the essential ubiquitin-specific protease USP8 ([10] and references therein), which modulate the balance between recycling of the deubiquitinated proteins back to the cell surface and their trafficking towards lysosomes after transiting through multivesicular bodies (MVBs), allowing signal desensitization through receptor degradation.

Endocytosis and MVB biogenesis largely rely on the conserved Endosomal Sorting Complex Required for Transport (ESCRT) machinery [3], which is also involved in many other membrane remodeling processes (reviewed in [29]). The ESCRT machinery consists of five complexes, ESCRT-0, -I, -II, -III and VPS4, that act sequentially at the endosomal membrane during the intracellular trafficking of endocytosed membrane

Abbreviations: ACTH, Adenocorticotrophin hormone; CD, Cushing's disease; DUB, deubiquitinating enzyme; ESCRT, Endosomal Sorting Complex Required for Transport; EGF, Epithelial Growth Factor; EGFR, Epithelial Growth Factor Receptor; HTRF®, Homogeneous Time-Resolved Fluorescence; HTS, high-throughput screening; MIM, MIT Interacting Motif; MIT, Microtubule Interacting and Trafficking domain; PPI, protein-protein interaction; TR-FRET, Time-Resolved Fluorescence Resonance Energy Transfer; WT, Wild-Type.

* Corresponding author at: Univ. Grenoble Alpes, CEA, Inserm, IRIG, BGE, CEA-Grenoble, 17 avenue des Martyrs, Cedex 9, F-38000 Grenoble, France.
E-mail address: marie-odile.fauvarque@cea.fr (M.-O. Fauvarque).

https://doi.org/10.1016/j.slasd.2022.08.003
Received 16 June 2022; Received in revised form 6 July 2022; Accepted 15 August 2022
Available online 20 August 2022

cargoes. Following the clustering of the internalized ubiquitinated cargoes on the early endosomes, ESCRT-0, -I and –II initiate membrane bending and ESCRT-III and VPS4 further direct membrane fission resulting in the release of cargo-containing intraluminal vesicles (ILVs) in the forming MVBs [11,20,31]. Dynamics of the ESCRT machinery involve the successive formation and disassembly of a variety of oligomeric complexes through multiple protein-protein interaction events. Major complexes formation implies Microtubule Interacting and Trafficking (MIT) domains on effector proteins, such as VPS4 or USP8, and MIT Interacting Motifs (MIM) present on ESCRT-III proteins [7,24,27].

In the context of EGF stimulation, the MIT domain of USP8 is required for its interaction with ESCRT proteins, association with endosomal membranes and appropriate EGFR sorting [24]. Moreover, EGF stimulation induces a rapid and transient ubiquitination of CHMP1B that is critical for physiological endocytic trafficking and signal regulation after EGFR activation [8]. Indeed, mutation of the four lysine residues K49, K52, K87 and K90 (mutant CHMP1B-4K>R) was shown to strongly reduce CHMP1B ubiquitination and to perturb EGFR trafficking in human cells with a delayed internalization and a stabilization of the receptor at the plasma membrane. Remarkably, K87 and K90 residues are located in a region subjected to massive conformational changes during the closed/inactive to the open/active transition of CHMP1B [17]. Furthermore, mutation of the *Drosophila* endogenous *Chmp1* gene induces wing morphogenesis defects [28]. While the wild type (WT) human CHMP1B protein can rescue these defects, the mutated human protein CHMP1B-4K>R fails to do so, further indicating that these lysine residues are critical for CHMP1B function in a living organism [8].

Besides its established implication in the endocytic process, USP8 has recently arisen as a promising therapeutic target in at least two distinct pathological contexts associated with USP8 overexpression or gain-of-function variants. On the one hand, in lung cancer cells exhibiting chemoresistance to EGFR inhibitor-based treatments, overexpressed USP8 may favor the stabilization of EGFR and/or other RTKs [6,13]. On the other hand, genetic studies demonstrated that a strong proportion of patients with the Cushing's disease (CD) expresses gain-of-function variants of USP8 [14,16,22,23,30]. CD is a rare metabolic disorder where a pituitary corticotroph microadenoma secretes deregulated amounts of adenocorticotrophin hormone (ACTH). Here, the USP8-dependent EGFR stabilization would possibly induce enhanced expression of *POMC*, the gene encoding the ACTH precursor [21,23].

In the present work, we report the development of a quantitative Homogeneous Time-Resolved Fluorescence (HTRF®) energy transfer assay dedicated to the detection and monitoring of the interaction between USP8 and its endocytic substrate CHMP1B. This assay was performed directly on transfected cell lysates to detect the USP8::CHMP1B complex. It was further adapted on a robotic platform for the automated screening of the Fr-PPIChem chemical library of 10,314 compounds dedicated to target PPIs [5] with the aim of discovering inhibitors of this interaction. This screening campaign resulted in the selection of several compounds capable to block the USP8::CHMP1B interaction. In a second step, this HTRF® assay was adapted for assessing the impact of CHMP1B mutations on its interaction with USP8. We notably showed that two conserved leucine residues of the MIM domain (L192 and L195) known to mediate MIT::MIM interactions [4,15,26,33] are also required for USP8::CHMP1B interaction. By contrast, the four lysine residues undergoing ubiquitination are not necessary for this interaction, suggesting that substrate recognition of CHMP1B by USP8 is independent from its ubiquitinated status.

Materials and methods

Reagents

Europium (Eu) cryptate- or d2-conjugated mouse monoclonal antibodies anti-c-myc (anti-myc-Eu #61MYCKLA or anti-myc-d2 #61MYCDAA), and anti-HA (anti-HA-Eu #610HAKLA or anti-HA-d2 #610HADAA) were purchased from Cisbio (Perkin Elmer). For western and dot blots, the following antibodies were used: rat anti-HA (clone 3F10; Sigma-Aldrich; dilution 1:1000), mouse anti-myc (in-house supernatant from the ECACC hybridoma clone 9E10; 1:50), mouse anti-Flag® (clone M2; Sigma-Aldrich #F1804; 1:1000), rabbit anti-GFP (Cell Signaling #2555; 1:1000), goat HRP-conjugated anti-mouse IgG (Sigma-Aldrich #A4416; 1:5000), donkey HRP-conjugated anti-rat IgG (Jackson Immunoresearch #712-036-153; 1:5000) and goat HRP-conjugated TrueBlot® anti-rabbit IgG (Rockland; 1:1000). Protease inhibitors (#P8340), BSA, TX100, Tween 20, DMSO and propidium iodide (#P4864) were from Sigma-Aldrich. KF was from Acros Organics. Hepes was purchased from Thermofisher. The Fr-PPIChem [5] chemical library of 10,314 compounds was provided by the ANR PPIChem consortium (ANR #: ANR-15-CE18-0023). Selected chemical compounds were purchased from Ambinter. All PCR primers were purchased from Sigma-Aldrich or Eurofins (**Suppl. Table 1**). Restriction enzymes were from New England Biolabs.

DNA constructs

DNA fragments encoding human USP8 (from plasmid pCMV-FLAG-1 USP8, MRC, Dundee, UK), human CHMP1B (Genbank BC065933) and its mutants CHMP1B$^{\Delta\alpha4\alpha5\alpha6}$ [8], CHMP1B$^{\Delta MIM}$ (lacking residues 184-199), CHMP1B$^{L192D\text{-}L195D}$ and CHMP1B$^{L192A\text{-}L195A}$ were PCR-amplified from cDNA clones and inserted into the mammalian expression vectors pcDNA3.1 (Invitrogen) or pEGFP-C1 (Clontech). When needed, HA or myc N-terminal tags were added by intermediate subcloning steps. The complete inserts were sequenced by Genewiz or Eurofins Genomics. Plasmid DNAs were purified using Nucleospin Plasmid Quick Pure kits (Macherey-Nagel).

Cell culture and transfection

Human embryonic kidney 293T cells (HEK293T; American Type Culture Collection, CRL-11268) and HeLa cells (American Type Culture Collection, CCL-2) were maintained in Dulbecco's modified Eagle's medium (DMEM #31966-021; Gibco) supplemented with 10% heat inactivated fetal bovine serum (FBS; Hyclone) and 1% Penicillin/Streptomycin mix (Gibco), in a humid atmosphere with 5% CO_2 at 37 °C.

For transient transfection, HEK293T cells (≈ 70,000 cells per cm^2) were seeded in DMEM/10% FBS, in poly-L-lysine (Sigma-Aldrich)-coated microplates or Petri dishes (Falcon). After overnight growth, transfection was carried out using Fugene HD reagent (Promega), according to the manufacturer protocol, in the following conditions: 300 ng of total DNA in 15 μL of DNA:Fugene (1 µg:2 µL ratio) mix per cm^2. A molar ratio of 1:1 to 2:1 USP8:CHMP1B (WT or variant) encoding plasmids was usually used for co-transfections.

Preparation of cell lysates for HTRF® assays

Forty-eight hours after cell transfection, cells were rinsed in PBS (137 mM NaCl, 10 mM Na phosphate, 2.7 mM KCl, pH 7.4) and lysed in 75 μL/cm^2 of cold lysis buffer (1% Triton X-100 in 20 mM Tris, 150 mM NaCl, pH 7.4 (TBS)), supplemented with protease inhibitors for 30 min at 4 °C. Cell debris and nuclei / DNA were further disrupted by strong mixing on a cell disrupter (Disruptor Genie, Scientific industries) at 4 °C for 10 min, and pelleted at 20,000 x *g* for 5 to 15 min at 4 °C. The cleared lysates were stored frozen at -80 °C for up to six months. Usually, cell lysate replicates were produced from cells simultaneously transfected in three cell culture wells with the same DNA:Fugene mix.

Co-immunoprecipitation

HEK293T cells transiently expressing GFP-CHMP1B, GFP-CHMP1B$^{L192D\text{-}L195D}$ or GFP-CHMP1B$^{L192A\text{-}L195A}$ together with Flag-

USP8 or empty vector were lysed in 50 mM Tris pH 7.5, 150 mM NaCl, 1mM EDTA, 1% Triton X-100, 0.5% sodium deoxycholate plus protease inhibitors. Cleared lysates were incubated with anti-Flag® M2 agarose beads (Sigma-Aldrich) for 2 h. Beads were washed four times in the same buffer and resuspended in denaturing Laemmli buffer. Immunocomplexes were analyzed by western blot using mouse anti-Flag® and rabbit anti-GFP antibodies. Goat TrueBlot® anti-rabbit secondary antibodies were used to visualize GFP-CHMP1B proteins.

Western Blot

Cell lysates were subjected to electrophoresis on 4-15% gradient SDS-polyacrylamide gels (Stain free precast gels; Biorad). Proteins were transferred to PVDF membranes (Immobilon P, Millipore). Total proteins were visualized by stain free detection prior to transfer for comparison of sample loads, when necessary. After blocking in 5% nonfat dry milk or 3% BSA in TBS containing 0.05% Tween 20 (TBST) for 3 h at room temperature, membranes were incubated with primary antibodies overnight at 4 °C, in TBST containing either 2% nonfat dry milk or 1% BSA. After three washes of 10 min each in TBST, HRP-conjugated secondary antibodies were applied for 1 h. Membranes were extensively washed and signals resulting from the reaction with the Immobilon Forte Western HRP substrate (Millipore) were imaged with the ImageLab 6.0.1 software in a ChemiDoc imager (BioRad).

CHMP1B species quantification on dot blots

Dot blot quantification of WT or mutated forms of HA-CHMP1B was performed on transfected cell lysates serially diluted in PBS. Serial dilutions were loaded as spots of 2 to 4 µL on nitrocellulose membranes (Protran BA83, Whatman). Membranes were air dried, rinsed in PBS, and successively incubated with the anti-HA primary and anti-rat HRP-conjugated secondary antibodies, as described in the "Western blot" section. The intensity of the spots was quantified with the ImageLab 6.0.1 software and plotted against the corresponding undiluted lysate volume. Linear fit of the curves by GraphPad Prism 9.2.0 (GraphPad Software, La Jolla, CA) provided slope values proportional to the CHMP1B species concentrations in the tested cell lysates. These values were used for normalization.

HTRF® Assay

The assay was conducted in 384-well white, flat bottom, small volume, polystyrene microplates (Greiner, #784075). All optimization experiments were performed as dose-response experiments carried out in triplicates. Serial dilutions of cell lysates were prepared in lysis buffer and contained up to 10 µL of cell lysate in a total volume of 10 µL. These dilutions were mixed with 10 μL of the donor/acceptor antibody pair (anti-myc-Eu/anti-HA-d2 or anti-HA-Eu/anti-myc-d2), diluted as recommended by the manufacturer in HTRF® buffer (50 mM Hepes, pH 7.5, 0.4 M KF, 0.1% BSA, 0.05% Tween 20). The plates were then briefly centrifuged at 200 × g for 30 s in an Eppendorf 5810 centrifuge with the A-4-62 swinging-bucket rotor (Eppendorf). Each well fluorescence was recorded after 3 to 5 h of incubation at room temperature, using an Infinite M1000 microplate reader (Tecan). This time range was permitted by the HTRF® signal stability. Europium was used as TR-FRET donor and excited at 340 nm. d2 served as TR-FRET acceptor. Donor and acceptor emissions were acquired sequentially with a 60 μs delay after excitation, during a window time of 500 μs, at 620 and 665 nm, respectively.

Optimization of the assay and subsequent high-throughput screening of the Fr-PPIChem chemical library were carried out on cell lysates co-expressing myc-USP8 and WT HA-CHMP1B. The negative controls producing the background FRET signal were either the lysis buffer alone, or cell lysates prepared from myc-USP8 and HA-CHMP1B$^{\Delta\alpha4\alpha5\alpha6}$ co-transfected cells.

Quantitative HTRF® assay on CHMP1B variants

The assay was performed on a mix of lysates of cells transfected with myc-USP8 or with WT or mutant HA-CHMP1B constructs. Lysates were diluted in non-transfected cell lysate to keep the total protein concentration constant between samples. Serial dilutions of WT or mutant HA-CHMP1B lysates combined with a fixed amount of a myc-USP8 lysate in a final volume of 10 µL were pre-incubated at room temperature for 1 h to allow USP8::CHMP1B complex formation before conducting the HTRF® assay, using lysis buffer as negative control. The HTRF® signals were then normalized to the relative WT or mutant CHMP1B protein amount, as quantified by dot blot.

High-Throughput Screening (HTS) and validation of primary hits

Chemicals from the Fr-PPIChem were obtained as 1 mM solutions in 100% DMSO. They were diluted extemporaneously in lysis buffer at 50 µM to perform HTS on simplicates. The positive control was a cell lysate prepared from HA-CHMP1B and myc-USP8 co-transfected cells defining the highest signal for USP8::CHMP1B interaction (100% interaction). A lysate from cells co-transfected with the truncated HA-CHMP1B$^{\Delta\alpha4\alpha5\alpha6}$ construct and myc-USP8 was used as negative control producing the minimal background signal (no interaction). Both cell lysates were prepared in sufficient amount for the screening campaign and hit confirmation assays. Five microliters of the cell lysate adequately diluted in lysis buffer were pre-incubated for 10 min at RT with 5 µL of DMSO or compounds, prior to addition of 10 µL of the HTRF® paired antibodies. After 3 to 5 h at room temperature, each well fluorescence was recorded as described in the "HTRF® assay" section. All reagents were dispensed into the 384-well microplates using the robotic facilities of the CMBA platform (https://www.cea.fr/drf/IRIG/english/Pages/Platform/CMBA.aspx). Positive and negative control wells (32 of each per 384-well assay plate, homogeneously distributed in the two first and two last columns) contained 5% (v/v) DMSO. These controls were used for calculation of the statistical Z' factor (see "Data analysis" section) for each plate.

Data analysis

For each well, the HTRF® signal was expressed as a raw TR-FRET ratio: $R_{sample} = F_{665nm}/F_{620nm}$ x 10^4, where F_{xnm} is the fluorescence value read at a wavelength of x nm. The factor of 10^4 was used for easier reading. The signal was further transformed by background substraction and normalization, giving a percentage of ΔF: $\%\Delta F_{sample} = (R_{sample}\text{-}R_N)/R_N$ x 100, where R_N is the mean HTRF® signal from the negative control wells. Data reliability and robustness were evaluated by calculating the Z' factor [34] using the following formula: $Z' = 1 - 3 \times (\sigma_P + \sigma_N) / |R_P - R_N|$, where σ_P and σ_N (R_P and R_N) are the standard deviations (resp. means) for the HTRF® signal of the positive and negative controls of interaction, respectively. If higher than 0.5, this factor indicates that the difference between the responses given by negative and positive controls is high and reproducible enough to allow valid detection of bioactive compounds.

Screen data were analyzed using the in-house TAMIS software (https://www.bge-lab.fr/Pages/CMBA/TAMIS.aspx). Standard deviation and mean of the HTRF® signal for both controls as well as the Z' factor were calculated for each plate. The effect of a compound on the interaction was normalized to both controls, and expressed as a percentage of inhibition calculated as follows: $(\%\text{ of inhibition})_{compound} = 100 - (R_{compound} - R_N)/(R_P - R_N) \times 100$, where $R_{compound}$ is the HTRF® signal measured in the presence of the compound.

The software GraphPad Prism 9.2.0 was used to generate graphs and calculate IC50 values for inhibitory compounds applying a weighted four parameter logistic model regression analysis.

Primary hit selection and validation

The inhibition threshold for hit selection was determined with the TAMIS software as three times the standard deviation of the positive controls of interaction (0% inhibition). Among this first hit selection, compounds suspected to interfere with the HTRF® process, for example producing a saturating fluorescent signal at 620 nm, were retrieved as well as frequent hitters, *i.e.* molecules inducing more than 40% inhibition in at least four unrelated screening campaigns (Dr X. Morelli and Dr P. Roche, personal communication). The remaining compounds were ordered as powder (Ambinter, see **Suppl. Table 2**), and 10 mM stock solutions were prepared in 100% DMSO. Compounds were serially diluted in lysis buffer (8 points from 0.8 to 50 μM compound), and their inhibitory effect was tested in triplicates for each dilution on the lysate previously used for the screening campaign. Positive and negative controls containing 0.5% DMSO were included.

Cell growth and death analysis

The IncuCyte® ZOOM live-cell imaging system (Sartorius, Göttingen, Germany) was used for kinetic monitoring of cell growth and cytotoxicity evaluation. HeLa cells were seeded at 6,000 cells per well in 80 μL of fresh culture medium in microclear 96-well tissue culture microplates (Greiner, #655090) and incubated overnight at 37 °C in a humidified atmosphere (5% CO_2). Cellular toxicity was assessed using propidium iodide (PI) at 0.5 µg/ml final concentration in the presence of inhibitors tested at 8 concentrations from 0.39 to 50 µM or 0.25% DMSO as a control, in triplicates. Three images per well were automat-

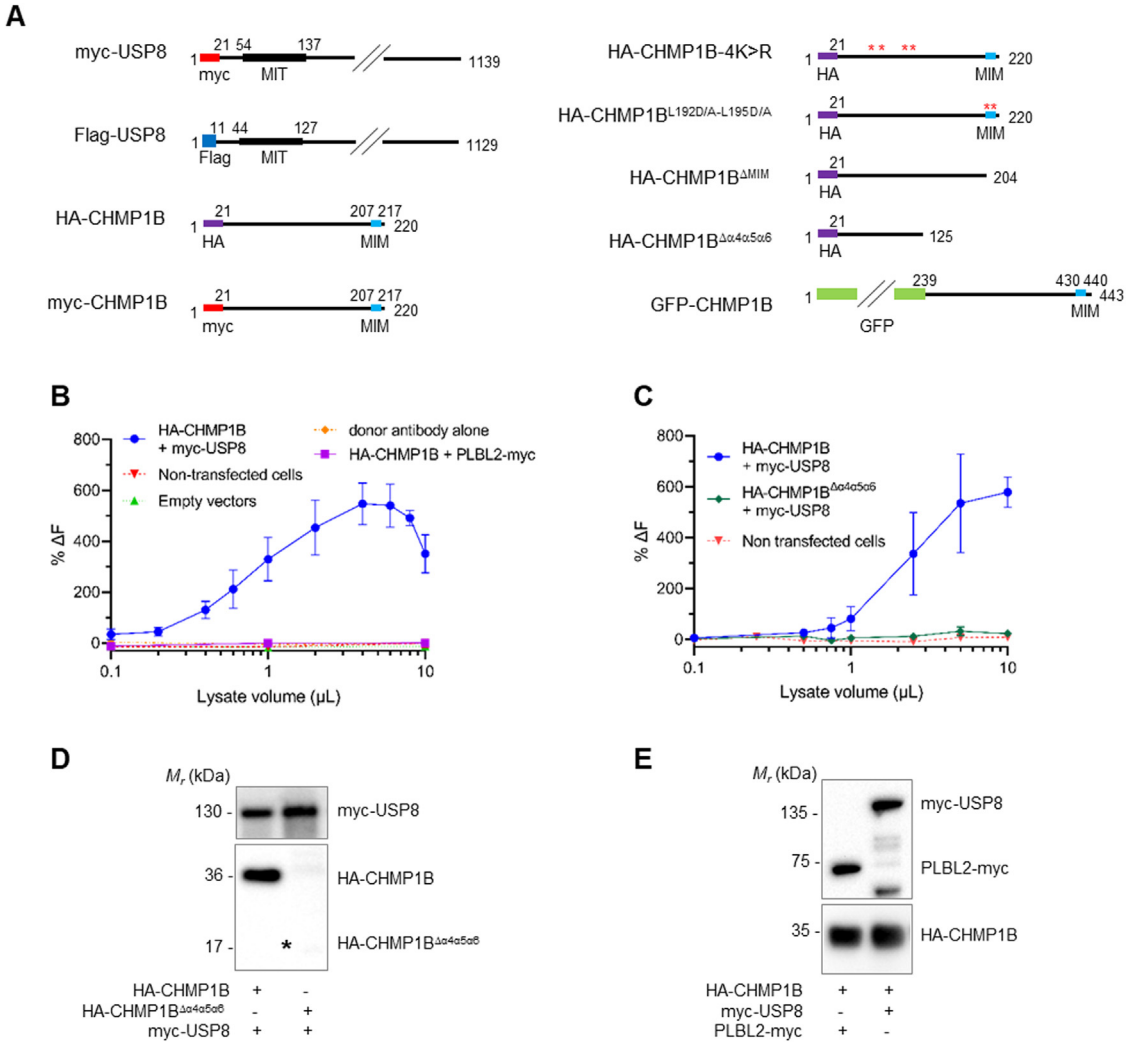

Fig. 1. Detection of the USP8::CHMP1B complex in lysates of co-transfected cells using the HTRF® technology. (A) Schematic representation of the constructs used in this study. The myc, HA and GFP tags, as well as the MIT and MIM domains are indicated with their respective position in the tagged proteins (amino acid residues numbering). Asterisks (*) indicate positions of the mutated residues. **(B to E) HEK293T cells transfected as indicated on each panel.** Co-transfection with HA-CHMP1B and myc-USP8 provides the positive control sample. The other conditions are negative controls: co-transfections with HA-CHMP1B and the non-relevant protein construct PLBL2-myc, HA-CHMP1B$^{\Delta\alpha4\alpha5\alpha6}$ and myc-USP8, or empty vectors, or no transfection. **(B and C) Typical HTRF® dose-response curves.** Serial dilutions corresponding to 0.1 to 10 µL of undiluted lysates were incubated with anti-myc-Eu and anti-HA-d2 antibodies for 4 h prior to fluorescence reading. Lysates of cells co-transfected with HA-CHMP1B and myc-USP8 were also assayed in the presence of the donor antibody anti-myc-Eu alone **(B)**, as another negative control. The curves represent the mean HTRF® signal detected for technical triplicates, using the lysis buffer as the background reference. **(D) Expression of the HA-CHMP1B$^{\Delta\alpha4\alpha5\alpha6}$ deletion mutant.** Cell lysates (3 µL for myc-USP8/HA-CHMP1B and 21 µL for myc-USP8/HA-CHMP1B$^{\Delta\alpha4\alpha5\alpha6}$) were analyzed by anti-HA or anti-myc immunoblotting. The HA-CHMP1B$^{\Delta\alpha4\alpha5\alpha6}$ protein is hardly detectable (asterisk *). **(E) Expression of the non-relevant PLBL2-myc protein.** Cell lysates were analyzed by anti-HA or anti-myc immunoblotting. PLBL2-myc is expressed in equivalent amounts as myc-USP8.

ically acquired every 4 h over a period of 60 h with a 10 × objective, in phase contrast and in the red fluorescence channel (PI staining). Phase contrast image analysis allows monitoring of cell growth (cell confluence % parameter). A threshold based on the fluorescence intensity of PI staining was applied for the selection of the PI^+ dead cells (PI^+ cell count parameter). The Area Under the Curve (AUC) was generated from each kinetic curve and condition in the open-source R studio software (https://www.rstudio.com/). The software GraphPad Prism 9.2.0 was used to generate graphs and calculate IC50 values for inhibitory compounds applying a weighted four parameter logistic model regression analysis.

Results

Assessing USP8::CHMP1B interaction by a quantitative HTRF® assay in cell lysates

In order to better characterize the USP8::CHMP1B interaction, and to search for chemical modulators thereof, we adapted the Homogeneous Time-Resolved Fluorescence (HTRF®) technology directly on lysates from cells co-expressing CHMP1B and USP8, each bearing a specific tag. In the final setup, the interaction between HA-CHMP1B and myc-USP8 (Fig. 1**A**) was detected by the means of anti-HA and anti-myc antibodies respectively coupled to Europium cryptate (fluorescence donor) and d2 (acceptor fluorophore). This interaction was robust and repeatedly observed in independent experiments (Figs. 1**B,C** and 2). The HTRF® signal obtained was dependent on the dose of the lysate and exhibited a hook effect at high lysate volumes, a phenomenon classically observed in immunoassays for analyte concentrations at which antibody amounts are limiting. Accordingly, increasing the antibody concentration slightly displaced this effect towards higher lysate amounts (**Suppl. Fig. S1A**). All negative controls tested (non-transfected cell lysates, or lysates from cells transfected with empty vectors, or use of the donor antibody alone) produced no signal regardless of the dose of lysate used, as did the lysis buffer used as a reference negative control (Fig. 1**B,C**). A truncated construct HA-CHMP1B$^{\Delta\alpha4\alpha5\alpha6}$ lacking the C-terminal part of CHMP1B that mediates its interaction with USP8 [8,24] failed to produce any signal (Fig. 1**C** and **Suppl. Fig. S1B**). Noteworthy, this truncated HA-CHMP1B$^{\Delta\alpha4\alpha5\alpha6}$ protein was hardly detectable in co-transfected cell lysates suggesting that it is unstable (Fig. 1**D**). Therefore, this control is rather similar to a negative control expressing myc-USP8 only. Co-transfection of either HA-CHMP1B or myc-CHMP1B with Flag-USP8 instead of myc-USP8 both led to a dose-dependent HTRF® signal, indicating that the nature of the tags was not critical for the interaction (**Suppl. Fig. S1B,C**). Conversely, lysates of cells co-expressing HA-CHMP1B and PLBL2-myc, the myc-tagged version of a non-relevant soluble lysosomal protein [12], did not produce any HTRF® signal in this assay (Fig. 1B,E). Taken together, these results indicate that the observed signal is attributable to a specific interaction between CHMP1B and USP8 and not to the associated HA and myc tags.

In conclusion, the HTRF® approach, commonly applied to purified proteins, was here used to detect the interaction between USP8 and CHMP1B directly in cell lysates. Our results both confirmed the capacity of USP8 to interact with the ESCRT protein CHMP1B and defined a specific assay to detect the USP8::CHMP1B interaction within cell lysates in a dose-dependent manner.

Selection of chemicals disrupting the USP8::CHMP1B complex in cell lysates

To identify compounds capable of disrupting the USP8::CHMP1B complex, we used the Fr-PPIChem [5] chemical library counting 10,314 small molecules specifically designed to target protein interfaces, that are dissolved in pure DMSO. No effect of DMSO in a range from 0.1 to 5% was observed on the intensity of the HTRF® signal, indicating that this solvent is compatible with the HTRF® test (Fig. 2**A**). For the screening campaigns, positive and negative controls of interaction

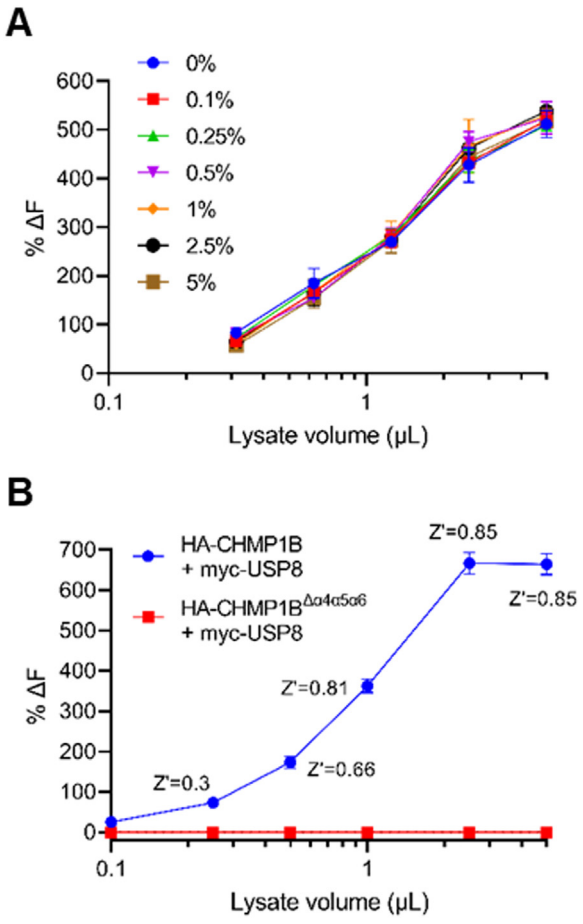

Fig. 2. Screening preliminary experiments. (A) DMSO tolerance of the HTRF® reaction. Serial dilutions corresponding to 0.3 to 10 µL of undiluted cell lysates from co-transfections of HEK293T cells with myc-USP8 and HA-CHMP1B constructs were tested by incubation with anti-myc-Eu and anti-HA-d2 antibodies in the presence of increasing concentrations of DMSO, for 4 h prior to fluorescence reading. The curves represent the mean HTRF® response of technical triplicates, using the lysis buffer as the background reference. One representative experiment out of three is shown. **(B) Dose-response analysis of the USP8::CHMP1B interaction in the lysate used for the screening campaign**. HEK293T cells were co-transfected with myc-USP8 and HA-CHMP1B or HA-CHMP1B$^{\Delta\alpha4\alpha5\alpha6}$ (negative control). Serial dilutions corresponding to 0.1 to 5 µL of the undiluted lysates were assayed in 32 technical replicates for determination of the Z' factor and of the optimal myc-USP8/HA-CHMP1B lysate amount to use for the screening of the Fr-PPIChem library.

were lysates of cells co-transfected respectively with both myc-USP8 and HA-CHMP1B constructs that produced the highest signal specific for the USP8::CHMP1B interaction, or with myc-USP8 and the non-interacting, deletion mutant HA-CHMP1B$^{\Delta\alpha4\alpha5\alpha6}$ that produced the minimal or background signal (Fig. 1**C**). Both cell lysates were prepared in quantities sufficient for the entire screening campaigns.

The statistical robustness of this HTRF® assay was validated by calculation of the Z' statistical factor [34] (See Materials and Methods). Briefly, after automation of the process on the robotic platform, a dose-response experiment was performed on serial dilutions (from 0.1 to 5 µL of undiluted lysate) of the positive and negative control lysates, using 32 replicates for each dilution (Fig. 2**B**). The calculated Z' factor for each volume of undiluted lysate was higher than 0.5 above 0.6 µL, and exceeded 0.8 for volumes greater than 1 µL, indicating that the assay is well suited for HTS. The classical HTRF® curve reached a maximum %ΔF of about 700% for 2.5 µL of the positive control lysate. Considering these data, the chemical library was screened using 2 µL of undiluted

cell lysate per sample leading to a high signal-to-background ratio while still in the linear part of the curve (0.81 < calculated Z' < 0.85).

The Fr-PPIChem library was then screened at the concentration of 50 μM using the same robotic protocol. One plate out of 33 (corresponding to 320 compounds) was excluded from the analysis due to technical problems during the screening campaign. The results were analyzed with the in-house TAMIS software (Fig. 3**A**). Z' factors values ranged from 0.63 to 0.81 (mean 0.74, SD 0.05, n = 32 plates; **Suppl. Fig. S2**). Thirty-one compounds inducing a signal inhibition above the 22% inhibition threshold were selected and filtered again to exclude frequent hitters and flagged compounds (see Material and Methods). This procedure led to the final selection of 19 primary hits. Selected compounds were prepared from fresh powders and tested at 50 μM and 10 μM in triplicates to confirm their ability to disrupt the USP8::CHMP1B complex. Five compounds were excluded after this secondary screening because they showed no robust inhibition. The inhibitory effect of the other 14 hits was further analyzed by dose-response HTRF® assays at compound concentrations ranging from 0.8 to 50 μM. Based on the results, the 14 confirmed hits were classified into three groups of maximum inhibitory capacity, corresponding to respectively high, medium and low inhibition (>60% inhibition, 30-60% inhibition, and <30% inhibition), with IC50s ranging from 2.1 μM to > 40 μM (average of two experiments; Fig. 3**B-D**). In this final step, three compounds (#15, 17 and 18) did not reach the primary screening threshold of 22% of inhibition while the other 11 compounds were considered as confirmed hits as they displayed robust inhibition of the USP8::CHMP1B interaction (see chemical structure for compounds # 2, 3, 4, 6, 8, 11 and 13 in Fig. 4**; Suppl. Table 2**). One analog of compound #4 present in the Fr-PPIChem displayed no inhibition of the USP8::CHMP1B interaction in the primary screen (**Suppl. Table 2**).

The most potent inhibitory compounds were tested in cell culture to assess their effect on cell growth and viability and define their maximal non-toxic dose for future studies in living cells. The confluence (growth) and propidium iodide incorporation (dead cells) were quantified in HeLa cells treated during 60 h with compounds #2, 3, and 4 at concentrations ranging from 0.39 to 50 μM (Fig. 5). Among the three molecules, compound #2 is the less toxic on HeLa cells with an IC50 higher than 30 μM whereas compounds #3 and 4 display moderate cell toxicity with a respective IC50s of 14.7 and 10.4 μM (mean of three independent experiments).

Two conserved leucine residues rather than CHMP1B ubiquitination state trigger CHMP1B binding to USP8

We next took advantage of the HTRF® assay to explore the consequences of mutations in CHMP1B on its capacity to bind USP8. As mentioned earlier, CHMP1B interaction with USP8 involves a C-terminal MIM-containing region covering the last three helices (α4α5α6) of the ESCRT protein, which mediates binding to the N-terminal MIT domain of USP8 [8,24]. Within the ESCRT machinery, MIM/MIT recognition supports several protein-protein interactions, as shown for example for the couples IST1/calpain7 [19], IST1/MITD1 [15], CHMP1B/VPS4B [26] or CHMP1B/LIP5 [25]. Moreover, structural and/or point mutation studies evidenced the role of conserved leucine residues within the MIM domain in the binding interface with the MIT domain. Substitution of leucine residues by aspartate or alanine residues abrogates or strongly interferes with MIT binding in the couples IST1/MITD1 [15], IST1/VPS4 [4], CHMP1B/VPS4B [26,33] or CHMP1B/Spastin [33]. By analogy, deletion of the MIM domain or point mutations of the conserved L192 and L195 leucine residues in CHMP1B should similarly affect the USP8::CHMP1B interaction. Co-immunoprecipitation experiments indeed confirmed that the substitution of leucine residues L192 and L195 from the MIM domain by either aspartate (CHMP1B$^{L192D\text{-}L195D}$) or alanine (CHMP1B$^{L192A\text{-}L195A}$) residues massively impaired the pull-down of GFP-tagged CHMP1B by Flag-USP8 (Fig. 6**A**).

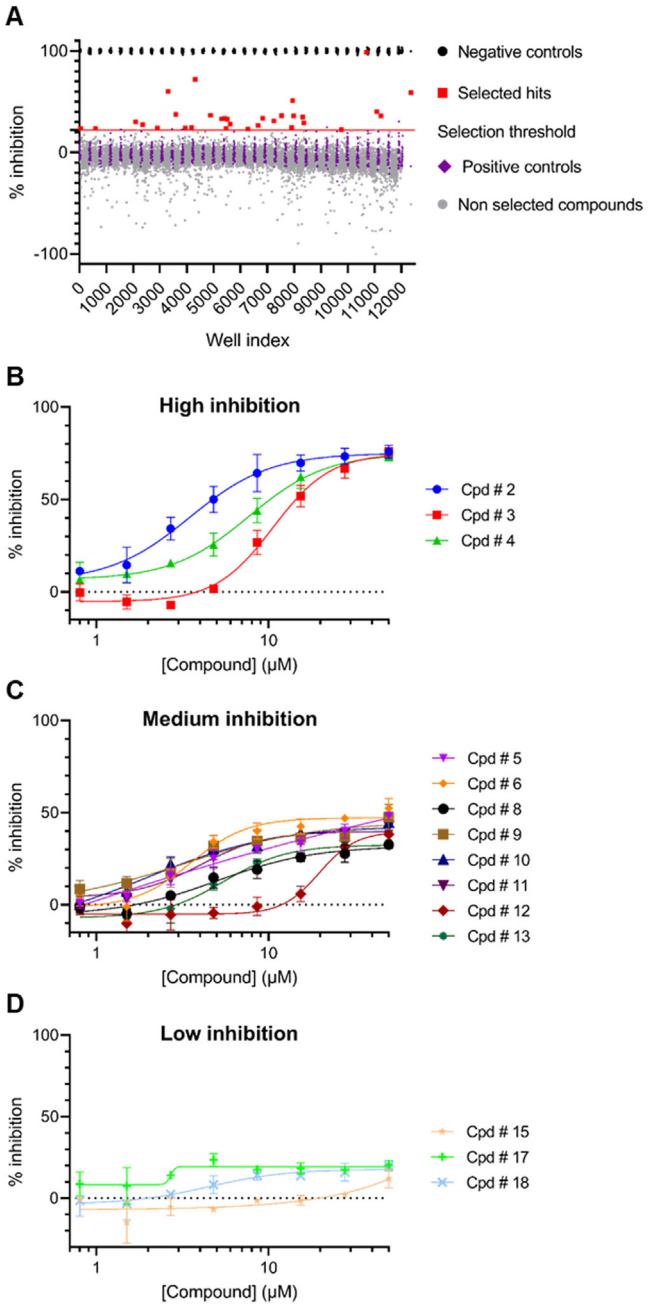

Fig. 3. Hit selection and confirmation from the Fr-PPIChem library. (A) Scatter plot of the percentage of inhibition of the Fr-PPIChem compounds. The hit threshold (3SD of the positive control of interaction) is equal to 22% of inhibition and corresponds to a hit rate of 0.31%. **(B to D) Inhibition curves of each selected hit.** The 14 molecules identified as inhibitors in the primary screen were tested in increasing concentrations (from 0.08 to 50 μM) in the HTRF® assay, in two microplates (z'=0.64 and 0.76, respectively). HTRF® signals were compared to that of a DMSO control to calculate a percentage of inhibition of the myc-USP8::HA-CHMP1B interaction. The curves were obtained as sigmoidal fit of technical triplicates. One representative experiment is shown out of two. Cpd: compound.

The HTRF® assay was then modified to analyze the interaction between USP8 and either CHMP1B-WT or CHMP1B$^{L192D\text{-}L195D}$ or two additional CHMP1B variants: a MIM domain-truncated CHMP1B (CHMP1B$^{\Delta MIM}$) and the CHMP1B-4K>R version of the protein. In preliminary experiments using HEK293T cells co-expressing myc-USP8 and the HA-CHMP1B variants, we observed a significant variation in the ex-

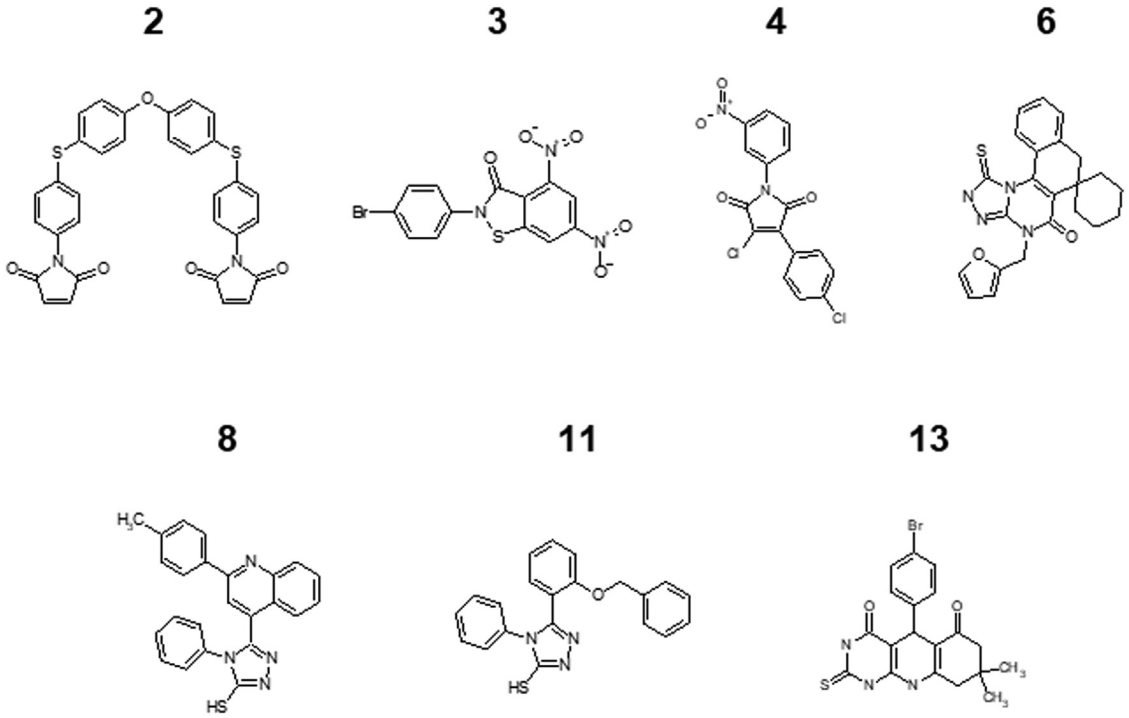

Fig. 4. Chemical structure of 7 confirmed hits.

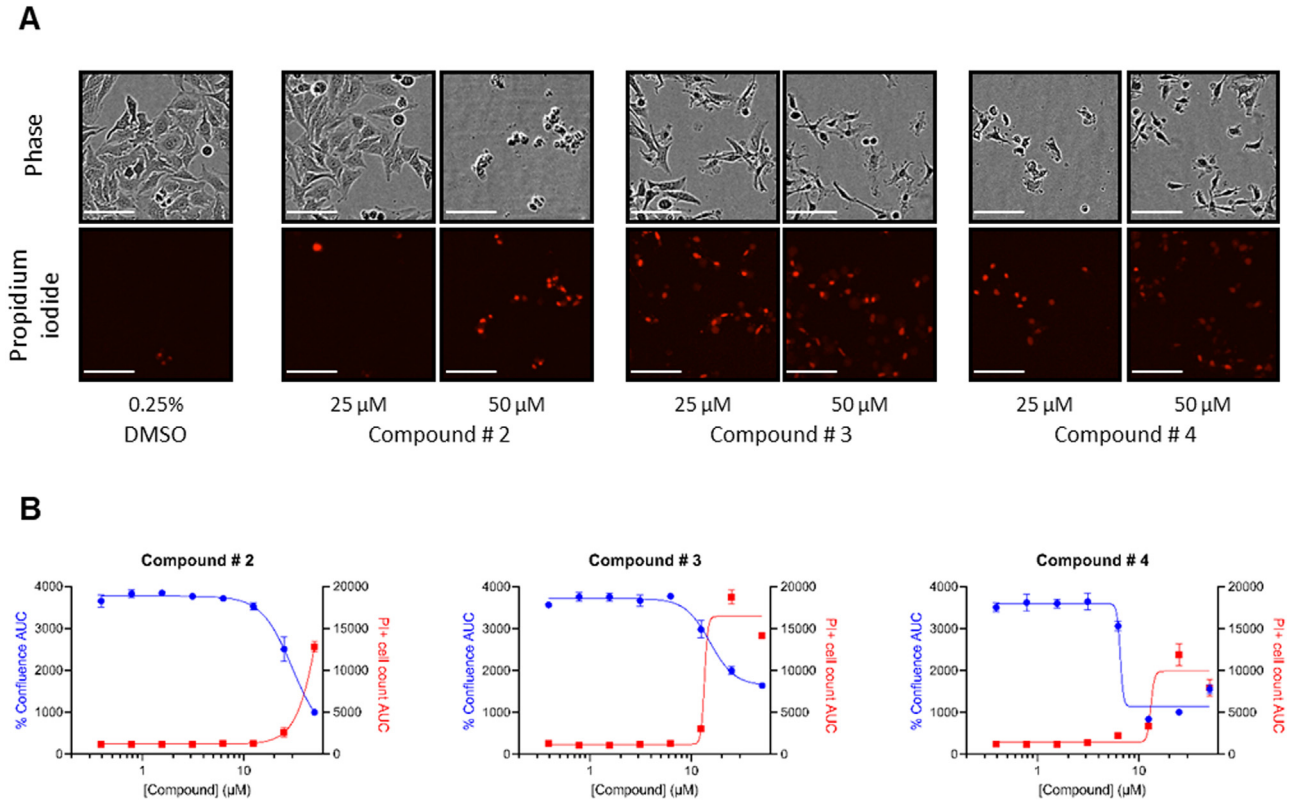

Fig. 5. Effect on cell growth and cytotoxicity of the three most potent hits. The effect of compounds # 2, 3 and 4 was evaluated on HeLa cells, by phase contrast (cell growth) and propidium iodide fluorescence (dead cells) imaging, every 4 h for a duration of 60 h. Compounds were tested in technical triplicates at eight concentrations from 0.39 to 50 µM. DMSO at 0.25% was used as a control. **(A) Phase contrast and fluorescence images taken after 60** h **of culture in presence of the molecules at 25** µ**M or 50** µ**M.** Scale bar: 100 µm. **(B) Confluence and death dose-response curves.** The Area Under the Curve (AUC) was generated from each kinetic curve and condition in the open-source R studio software (https://www.rstudio.com/). The curves shown are issued from one representative experiment out of three.

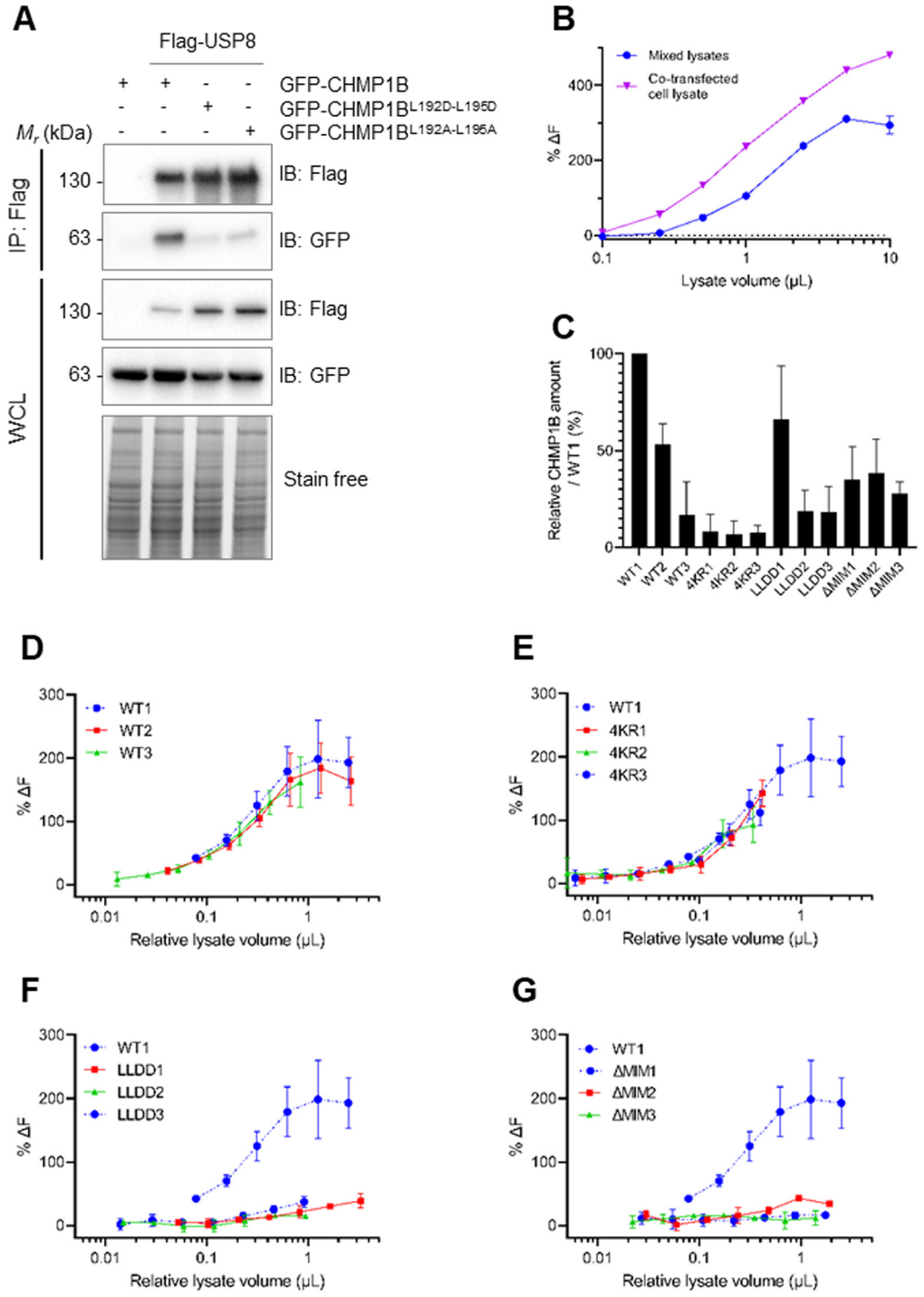

Fig. 6. CHMP1B mutants binding to USP8. (A) Co-immunoprecipitation of CHMP1B mutants with USP8. HEK293T cells were co-transfected with Flag-USP8 and GFP-CHMP1B, GFP-CHMP1B$^{L192D-L195D}$ or GFP-CHMP1B$^{L192A-L195A}$ constructs. Immunoprecipitation was carried out with the anti-Flag antibody. USP8 and CHMP1B proteins were revealed by western blot using respectively anti-Flag or anti-GFP antibodies. Total protein amount is shown. One representative experiment out of two is presented. **(B) USP8 and CHMP1B expressed in separate cell cultures can interact in mixed lysates.** Lysates of HEK293T cells overexpressing HA-CHMP1B or myc-USP8 were mixed in a 1:1 ratio and incubated for 1h prior to serial dilution in lysis buffer and monitoring of the protein interaction by HTRF® in technical triplicates. The resulting signal was compared to that of a lysate of cells co-expressing the two proteins. **(C) CHMP1B species relative expression**. Three replicate transfections of HEK293T cells were carried out for production of lysates for each HA-CHMP1B species. The amount of HA-CHMP1B (WT or mutant) expressed in cell lysates was plotted as a percentage of the WT HA-CHMP1B present in a reference lysate (WT1; mean +/- SD from 3 to 5 dot blot quantifications) (see **Suppl. Fig S4**). WT, wild-type CHMP1B; 4KR, CHMP1B-4K>R; LLDD, CHMP1B$^{L192D-L195D}$; ΔMIM, CHMP1B$^{\Delta MIM}$. **(D to G) Adjusted HTRF® dose-response curves of HA-CHMP1B species.** Serial dilutions of each HA-CHMP1B (WT or mutant) overexpressing cell lysate were mixed with a given amount of the myc-USP8 cell lysate. The HTRF® analysis of the USP8::CHMP1B interaction was carried out after 1 h incubation at room temperature. Dose-response curves were plotted as a function of the normalized HA-CHMP1B amount in the lysate (see **Suppl. Figure S4C,D**) . Each panel corresponds to one HA-CHMP1B species. **D**: wild-type (WT); **E**: CHMP1B-4K>R (4KR); **F**: CHMP1B$^{L192D-L195D}$ (LLDD); **G**: CHMP1B$^{\Delta MIM}$ (ΔMIM). The WT1 reference lysate curve is drawn on each graph for comparison. Each curve represents the mean of three independent HTRF® experiments, and three biological replicates were analyzed for each CHMP1B species.

pression level of the different CHMP1B constructs resulting in strong differences in the USP8/CHMP1B abundance ratio. Such variations made it impossible to compare CHMP1B variant properties regarding USP8 binding on single samples. To get around this problem, we first assessed if myc-USP8::HA-CHMP1B complexes can form after mixing individual lysates from cells expressing separately each of the two proteins USP8 or CHMP1B. We indeed observed a dose-dependent HTRF® signal very similar to that observed with a doubly transfected cell lysate indicating that the USP8::CHMP1B complex properly forms *ex cellulo* (Fig. 6**B**). Thus, aiming at a better control of the USP8/CHMP1B ratio in the samples assayed by HTRF®, cells were separately transfected with either myc-USP8 or one of the HA-CHMP1B constructs (WT or one of the mutants HA-CHMP1B-4K>R, HA-CHMP1B$^{L192D-L195D}$ and HA-CHMP1B$^{\Delta MIM}$). This strategy allowed to fix the amount of myc-USP8 present in each HTRF® assay while changing the amount of HA-CHMP1B lysate (**Suppl. Fig. S3A**). For each HA-CHMP1B construct, triplicates of cell lysates were prepared in three sets of independent transfections, and for each cell lysate, the HA-CHMP1B abundance was normalized to that of a reference lysate containing WT HA-CHMP1B (WT1) by dot blot quantification (**Suppl. Fig. S3B-D** and Fig. 6**C**).

The HTRF® results of three independent experiments were plotted against the normalized amount of HA-CHMP1B (Fig. 6**D-G**). These experiments revealed that deletion of the MIM domain of CHMP1B totally abolished CHMP1B interaction with myc-USP8, as expected. In agreement with the co-immunoprecipitation experiment results, only a very weak HTRF® signal was obtained with the CHMP1B$^{L192D-L195D}$ protein (about 15% of the WT signal), indicating that interaction with USP8 is massively, even if not completely, affected by the mutation of the two leucine residues. In contrast, the mutation of the ubiquitinated lysine residues in CHMP1B-4K>R did not affect the ability of the protein to interact with myc-USP8, indicating that ubiquitination of the CHMP1B substrate, at least on these particular sites, is not a prerequisite for binding to USP8.

Discussion

This work confirms the interaction between the deubiquitinase USP8 and the ESCRT-III component CHMP1B and establishes a statistically robust HTRF® assay allowing its detection and quantification in cell lysates. We demonstrate that this complex forms both in lysates from cells co-expressing the two proteins and *in vitro*, in mixes of lysates from cells transfected with each individual protein construct. The fact that the USP8::CHMP1B complex forms when mixing cell lysates indicates that the induction of the endocytic process is not a prerequisite for this interaction to occur, at least in overexpression conditions.

We demonstrated the requirement of the C-terminal MIM domain of CHMP1B and in particular, of conserved leucine residues in this motif in the formation of the USP8::CHMP1B complex, as anticipated from previous studies on other MIM/MIT domain pairs. These leucine residues L192 and L195 were previously shown to mediate CHMP1B interaction with VPS4B [26,33], Spastin [33] and Ist1 [32] suggesting a competition between CHMP1B partners for binding the CHMP1B MIM interface. Mutation of four lysine residues triggering ubiquitination of CHMP1B did not affect the ability of the protein to interact with USP8, indicating that ubiquitination of the CHMP1B substrate may not be required for CHM1P1B substrate recognition by USP8. This methodological approach may be extended to the analysis of USP8 interactions with other partners, such as Ist1 [1] or 14-3-3 [18], an adaptor protein that functions as a negative regulator of the deubiquitinase.

Using the HTRF® assay, we screened 9,994 compounds out of a dedicated library of 10,314 compounds specifically designed by *in silico* methods to target hydrophobic protein sequences and therefore PPI interfaces [5]. This screen resulted in the identification of a final set of 11 confirmed hits able to disrupt at various extents the USP8::CHMP1B complex previously formed in living cells. A review of these hits on the PubChem website (https://pubchem.ncbi.nlm.nih.gov/) revealed that patents related to resin manufacturing have been deposited for compound #2 while compounds #3 and 9 have been found active in other bioassays, targeting a wide array of proteins in the case of compound #3. According to Bosc and collaborators [5], the activity rate of the FR-PPIChem library in this particular screen for PPI inhibitors would be about 10 times higher than might be expected for a random library (*i.e* ~0,1% vs less than 0,01%), although this value must be taken with caution as different interfaces may lead to different values of activity rate. Such compounds could serve as chemical tools for the dynamic analysis of the role of USP8::CHMP1B complex in endocytosis without interfering with the catalytic-dependent functions of USP8 on many substrates.

Inhibiting USP8 catalytic activity has been proposed in several studies as a powerful mean to control cell proliferation or ACTH secretion in therapeutic perspectives for treating cancers or Cushing's disease [2,6,13,14]. The finding of chemicals that prevent the formation of active USP8-protein complexes may open new avenues in the design of alternative therapeutic strategies. Such compounds may indeed bind USP8 and either prevent USP8-dependent pathological outcomes (without affecting its overall functions) or be developed as tools for inducing targeted protein degradation. The chemical library screen presented in this study is part of this approach. It allowed successful selection of several specific inhibitors of the USP8::CHMP1B interaction that were not selected on several other PPIs, therefore bringing the proof of concept that breaking this interface in a specific manner is a reachable goal and may lead to the discovery of USP8 specific chemical binders in the near future. This approach, which is based on the quantification of the interaction between two proteins directly in a cell lysate, could be used not only for the identification of inhibitors but also for the identification of stabilizers of all kinds of protein complexes.

Declaration of Competing Interest

The authors declare that they have no known competing financial interests or personal relationships that could have appeared to influence the work reported in this paper.

Funding

This work was supported by the National Research Agency (Grants # ANR-15-CE18-0023 and ANR-21-CE18-0048-01 to Dr Fauvarque), the LabEX GRAL (Grenoble Alliance for Integrated Structural and Cell Biology), a program of the Chemistry Biology Health Graduate School of Université Grenoble Alpes (ANR-17-EURE-0003). Part of this work has been performed at the CMBA platform - IRIG-DS-BGE-Gen&Chem-CMBA, CEA-Grenoble, F-38054 Grenoble (a member of GIS-IBISA and ChemBioFrance National Research Infrastructure).

Acknowledgments

The authors thank Dr X. Morelli and Dr P. Roche (CRCM, Marseille), Dr F. Borel (IBS, Grenoble) and Dr D. Roche (Edelris S.A.S) for valuable discussion, information sharing, and selection of the compounds presented in this study.

Supplementary materials

Supplementary material associated with this article can be found, in the online version, at doi:10.1016/j.slasd.2022.08.003.

References

[1] Agromayor M, Carlton JG, Phelan JP, Matthews DR, Carlin LM, Ameer-Beg S, Bowers K, Martin-Serrano J. Essential role of hIST1 in cytokinesis. Mol Biol Cell 2009;20(5):1374–87.

[2] Albani A, Perez-Rivas LG, Reincke M, Theodoropoulou M. Pathogenesis of cushing disease: an update on the genetics of corticotropinomas. Endocr Pract 2018;24(10):907–14.
[3] Babst M. MVB vesicle formation: ESCRT-dependent, ESCRT-independent and everything in between. Curr Opin Cell Biol 2011;23(4):452–7.
[4] Bajorek M, Morita E, Skalicky JJ, Morham SG, Babst M, Sundquist WI. Biochemical analyses of human IST1 and its function in cytokinesis. Mol Biol Cell 2009;20(5):1360–73.
[5] Bosc N, Muller C, Hoffer L, Lagorce D, Bourg S, Derviaux C, Gourdel ME, Rain JC, Miller TW, Villoutreix BO, Miteva MA, Bonnet P, Morelli X, Sperandio O, Roche P. Fr-PPIChem: an academic compound library dedicated to protein-protein interactions. ACS Chem Biol 2020;15(6):1566–74.
[6] Byun S, Lee SY, Lee J, Jeong CH, Farrand L, Lim S, Reddy K, Kim JY, Lee MH, Lee HJ, Bode AM, Won Lee K, Dong Z. USP8 is a novel target for overcoming gefitinib resistance in lung cancer. Clin Cancer Res 2013;19(14):3894–904.
[7] Ciccarelli FD, Proukakis C, Patel H, Cross H, Azam S, Patton MA, Bork P, Crosby AH. The identification of a conserved domain in both spartin and spastin, mutated in hereditary spastic paraplegia. Genomics 2003;81(4):437–41.
[8] Crespo-Yanez X, Aguilar-Gurrieri C, Jacomin AC, Journet A, Mortier M, Taillebourg E, Soleilhac E, Weissenhorn W, Fauvarque MO. CHMP1B is a target of USP8/UBPY regulated by ubiquitin during endocytosis. PLoS Genet 2018;14(6):e1007456.
[9] Critchley WR, Pellet-Many C, Ringham-Terry B, Harrison MA, Zachary IC, Ponnambalam S. Receptor tyrosine kinase ubiquitination and de-ubiquitination in signal transduction and receptor trafficking. Cells 2018;7(3).
[10] Dufner A, Knobeloch KP. Ubiquitin-specific protease 8 (USP8/UBPy): a prototypic multidomain deubiquitinating enzyme with pleiotropic functions. Biochem Soc Trans 2019;47(6):1867–79.
[11] Henne WM, Stenmark H, Emr SD. Molecular mechanisms of the membrane sculpting ESCRT pathway. Cold Spring Harb Perspect Biol 2013;5(9).
[12] Jensen AG, Chemali M, Chapel A, Kieffer-Jaquinod S, Jadot M, Garin J, Journet A. Biochemical characterization and lysosomal localization of the mannose-6-phosphate protein p76 (hypothetical protein LOC196463). Biochem J 2007;402(3):449–58.
[13] Jeong CH. Inhibition of Ubiquitin-specific Peptidase 8 Suppresses Growth of Gefitinib-resistant Non-small Cell Lung Cancer Cells by Inducing Apoptosis. J Cancer Prev 2015;20(1):57–63.
[14] Jian F, Cao Y, Bian L, Sun Q. USP8: a novel therapeutic target for Cushing's disease. Endocrine 2015;50(2):292–6.
[15] Lee S, Chang J, Renvoise B, Tipirneni A, Yang S, Blackstone C. MITD1 is recruited to midbodies by ESCRT-III and participates in cytokinesis. Mol Biol Cell 2012;23(22):4347–61.
[16] Ma ZY, Song ZJ, Chen JH, Wang YF, Li SQ, Zhou LF, Mao Y, Li YM, Hu RG, Zhang ZY, Ye HY, Shen M, Shou XF, Li ZQ, Peng H, Wang QZ, Zhou DZ, Qin XL, Ji J, Zheng J, Chen H, Wang Y, Geng DY, Tang WJ, Fu CW, Shi ZF, Zhang YC, Ye Z, He WQ, Zhang QL, Tang QS, Xie R, Shen JW, Wen ZJ, Zhou J, Wang T, Huang S, Qiu HJ, Qiao ND, Zhang Y, Pan L, Bao WM, Liu YC, Huang CX, Shi YY, Zhao Y. Recurrent gain-of-function USP8 mutations in Cushing's disease. Cell Res 2015;25(3):306–17.
[17] McCullough J, Clippinger AK, Talledge N, Skowyra ML, Saunders MG, Naismith TV, Colf LA, Afonine P, Arthur C, Sundquist WI, Hanson PI, Frost A. Structure and membrane remodeling activity of ESCRT-III helical polymers. Science 2015;350(6267):1548–51.
[18] Meijer IM, Kerperien J, Sotoca AM, van Zoelen EJ, van Leeuwen JE. The Usp8 deubiquitination enzyme is post-translationally modified by tyrosine and serine phosphorylation. Cell Signal 2013;25(4):919–30.
[19] Osako Y, Maemoto Y, Tanaka R, Suzuki H, Shibata H, Maki M. Autolytic activity of human calpain 7 is enhanced by ESCRT-III-related protein IST1 through MIT-MIM interaction. FEBS J 2010;277(21):4412–26.
[20] Peel S, Macheboeuf P, Martinelli N, Weissenhorn W. Divergent pathways lead to ESCRT-III-catalyzed membrane fission. Trends Biochem Sci 2011;36(4):199–210.
[21] Perez-Rivas LG, Reincke M. Genetics of Cushing's disease: an update. J Endocrinol Invest 2016;39(1):29–35.
[22] Perez-Rivas LG, Theodoropoulou M, Puar TH, Fazel J, Stieg MR, Ferrau F, Assie G, Gadelha MR, Deutschbein T, Fragoso MC, Kusters B, Saeger W, Honegger J, Buchfelder M, Korbonits M, Bertherat J, Stalla GK, Hermus AR, Beuschlein F, Reincke M. Somatic USP8 mutations are frequent events in corticotroph tumor progression causing Nelson's tumor. Eur J Endocrinol 2018;178(1):57–63.
[23] Reincke M, Sbiera S, Hayakawa A, Theodoropoulou M, Osswald A, Beuschlein F, Meitinger T, Mizuno-Yamasaki E, Kawaguchi K, Saeki Y, Tanaka K, Wieland T, Graf E, Saeger W, Ronchi CL, Allolio B, Buchfelder M, Strom TM, Fassnacht M, Komada M. Mutations in the deubiquitinase gene USP8 cause Cushing's disease. Nat Genet 2015;47(1):31–8.
[24] Row PE, Liu H, Hayes S, Welchman R, Charalabous P, Hofmann K, Clague MJ, Sanderson CM, Urbe S. The MIT domain of UBPY constitutes a CHMP binding and endosomal localization signal required for efficient epidermal growth factor receptor degradation. J Biol Chem 2007;282(42):30929–37.
[25] Shim S, Merrill SA, Hanson PI. Novel interactions of ESCRT-III with LIP5 and VPS4 and their implications for ESCRT-III disassembly. Mol Biol Cell 2008;19(6):2661–72.
[26] Stuchell-Brereton MD, Skalicky JJ, Kieffer C, Karren MA, Ghaffarian S, Sundquist WI. ESCRT-III recognition by VPS4 ATPases. Nature 2007;449(7163):740–4.
[27] Tsang HT, Connell JW, Brown SE, Thompson A, Reid E, Sanderson CM. A systematic analysis of human CHMP protein interactions: additional MIT domain-containing proteins bind to multiple components of the human ESCRT III complex. Genomics 2006;88(3):333–46.
[28] Valentine M, Hogan J, Collier S. The Drosophila Chmp1 protein determines wing cell fate through regulation of epidermal growth factor receptor signaling. Dev Dyn 2014;243(8):977–87.
[29] Vietri M, Radulovic M, Stenmark H. The many functions of ESCRTs. Nat Rev Mol Cell Biol 2020;21(1):25–42.
[30] Wanichi IQ, de Paula Mariani BM, Frassetto FP, Siqueira SAC, de Castro Musolino NR, Cunha-Neto MBC, Ochman G, Cescato VAS, Machado MC, Trarbach EB, Bronstein MD, Fragoso M. Cushing's disease due to somatic USP8 mutations: a systematic review and meta-analysis. Pituitary 2019;22(4):435–42.
[31] Wollert T, Hurley JH. Molecular mechanism of multivesicular body biogenesis by ESCRT complexes. Nature 2010;464(7290):864–9.
[32] Xiao J, Chen XW, Davies BA, Saltiel AR, Katzmann DJ, Xu Z. Structural basis of Ist1 function and Ist1-Did2 interaction in the multivesicular body pathway and cytokinesis. Mol Biol Cell 2009;20(15):3514–24.
[33] Yang D, Rismanchi N, Renvoise B, Lippincott-Schwartz J, Blackstone C, Hurley JH. Structural basis for midbody targeting of spastin by the ESCRT-III protein CHMP1B. Nat Struct Mol Biol 2008;15(12):1278–86.
[34] Zhang JH, Chung TD, Oldenburg KR. A simple statistical parameter for use in evaluation and validation of high throughput screening assays. J Biomol Screen 1999;4(2):67–73.